Supplementary Information

A lithium-ion-active aerolysin nanopore for effectively trapping long single-stranded DNA

Zheng-Li Hu, Meng-Yin Li, Shao-Chuang Liu, Yi-Lun Ying* and Yi-Tao Long

Key Laboratory for Advanced Materials, School of Chemistry & Molecular Engineering, East China University of Science and Technology, Shanghai 200237, P. R. China.

* To whom correspondence should be addressed: yilunying@ecust.edu.cn

Table of Contents

Experimental Section

Reagents and Chemicals. Proaerolysin was prepared according to our previous work and activated by digestion with trypsin for four hours at room temperature.[1,2] The α-hemolysin was purchased from Sigma-Aldrich (St. Louis, MO, USA) and used without further purification. Trypsin-EDTA and decane (anhydrous, ≥ 99%) were purchased from Sigma-Aldrich (St. Louis, MO, USA). 1,2-Diphytanoyl-sn-glycero-3-phosphocholine (chloroform, ≥ 99%) was purchased from Avanti Polar Lipids Inc. (Alabaster, AL, USA). The sequence of the 102-nt DNA (ssDNA_102) is 5'-T_{40}-ACAGGCCGGGACAAGTGCAATA-T_{40}-3'. All single-strand DNA (ssDNA) samples were synthesized and HPLC-purified by Sangon Biotech Co., Ltd (Shanghai, China). All reagents and chemicals were of analytical grade. All solutions for analytical studies were prepared with ultrapure water (18.2 MΩ cm at 25°C) using a Milli-Q System (EMD Millipore, Billerica, MA, USA).

Electrical Recording. All the nanopore experiments were carried out at 22 ± 2 °C. The single-channel recordings were performed according to our previous studies.[2,3] A planar lipid bilayer was formed by applying 30 mg/mL diphytanoyl-phosphatidyl-choline in decane to a 50 μm orifice in a Delrin bilayer cup (Warner Instruments, Hamden, CT, USA). The planar bilayer apparatus was assembled by *trans* and *cis* chambers, each filled with 1 mL of electrolyte consisting of 1.0 M M^+Cl^- ($M^+ = K^+$ or Li^+), 10 mM Tris, 1.0 mM EDTA, pH 8.0. The aerolysin (AeL) or α-hemolysin (α-HL) was added to the grounded *cis* chamber, and pore insertion was determined by a well-defined jump in current value. Once a stable single-pore insertion was detected, the single-strand DNA (ssDNA) samples were added to the *cis* chamber at a final concentration of 2.0 μM. The current was detected with a pair of Ag/AgCl electrodes, recorded with a patch-clamp amplifier (Axopatch 200B, Axon Instruments, Forest City, CA, USA), filtered with an internal low-pass Bessel filter at 5kHz, and then digitized with a Digidata 1440A A/D converter at a sampling rate of 250 kHz by running the Clampex 10.4 software (Molecular Devices, USA). The data analysis was performed by an homemade software,[4,5] Clampfit 10.4 (Axon Instruments, Forest City, CA, USA) and OriginLab 8.0 (OriginLab Corporation, Northampton, MA, USA).

Molecular dynamics simulations. The structure of the wild-type (WT) AeL was obtained from the Protein Data Bank (entry 5JZT).[6] The nanopore-lipid system was constructed according to our previous work.[7] The cations (K^+ or Li^+) and Cl^- were added to balance the charges of AeL nanopore and achieve a concentration of 1 M. All

molecular dynamics (MD) simulations performed using NAMD,[8] the CHARMM36 force field,[9] 2 fs-integration time step, a 12 Å cutoff for van der Waals energies and the particle-mesh-Ewald (PME) method to treat long-range electrostatics.[10] For NPT simulations, the temperature was kept at 295 K using Langevin dynamics and the pressure was controlled at 1 atm with a Nosé-Hoover Langevin piston.[11] Following a 5000-step minimization, the AeL system was equilibrated in the NPT ensemble for 2 ns with the restrained heavy atoms (non-hydrogen) of protein and the relaxed water, lipid and hydration atoms. Then, the alpha carbons of the AeL protein were restrained and the equilibration simulation sustained 10 ns. Next, after removing all the restraints, the system was relaxed for 40 ns. According to the previous work,[12] the electrostatic potential distribution was obtained by averaging over the last 10 ns simulation trajectory using the PME electrostatics plugin of VMD.[13] The cations (K^+ or Li^+) are defined as being bound to AeL within a cutoff distance of 3.1 Å from the heavy atoms of the pore.[14] The binding number of K^+/Li^+ was evaluated by averaging over each frame during the last 10 ns equilibration.

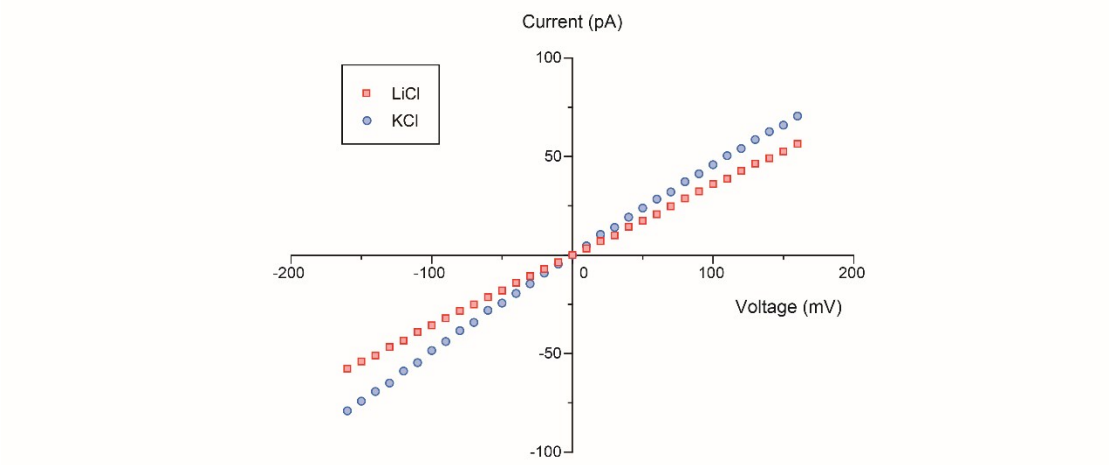

Fig. S1 *I-V* curves of a single aerolysin nanopore in LiCl (red squares) and KCl (blue circles). Data were obtained in 1.0 M M^+Cl^- (M^+ = Li^+, K^+), 10 mM Tris, 1.0 mM EDTA, pH 8.0 without any analytes in either side of the aerolysin nanopore.

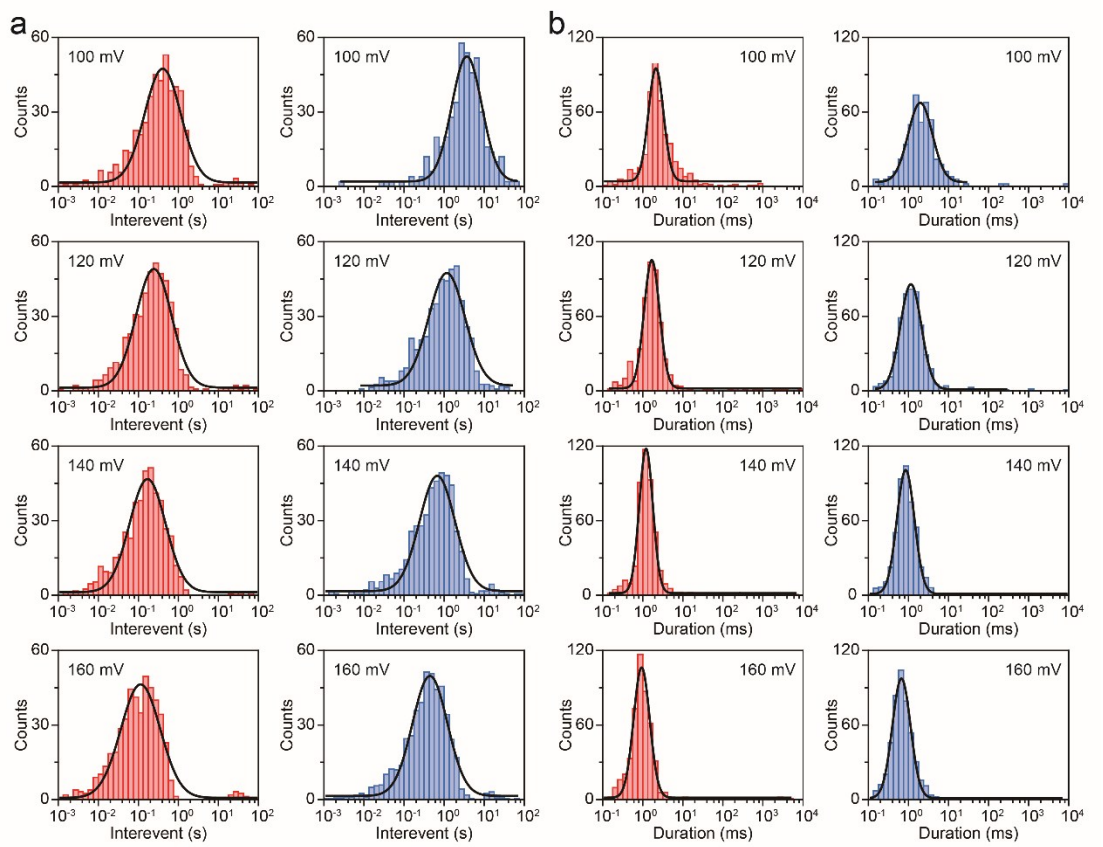

Fig. S2 Histograms of (a) event frequencies and (b) durations for a 102-nt ssDNA (ssDNA_102) in LiCl (red) and KCl (blue) at various voltages ranging from 100 to 160 mV, respectively (from top to bottom). The duration and frequency distributions are fitted to modified single-exponential functions. Data were obtained in 1.0 M M^+Cl^- (M^+ = Li^+ or K^+), 10 mM Tris, 1.0 mM EDTA, pH 8.0 with 2.0 μM ssDNA_102 in cap side of the aerolysin nanopore.

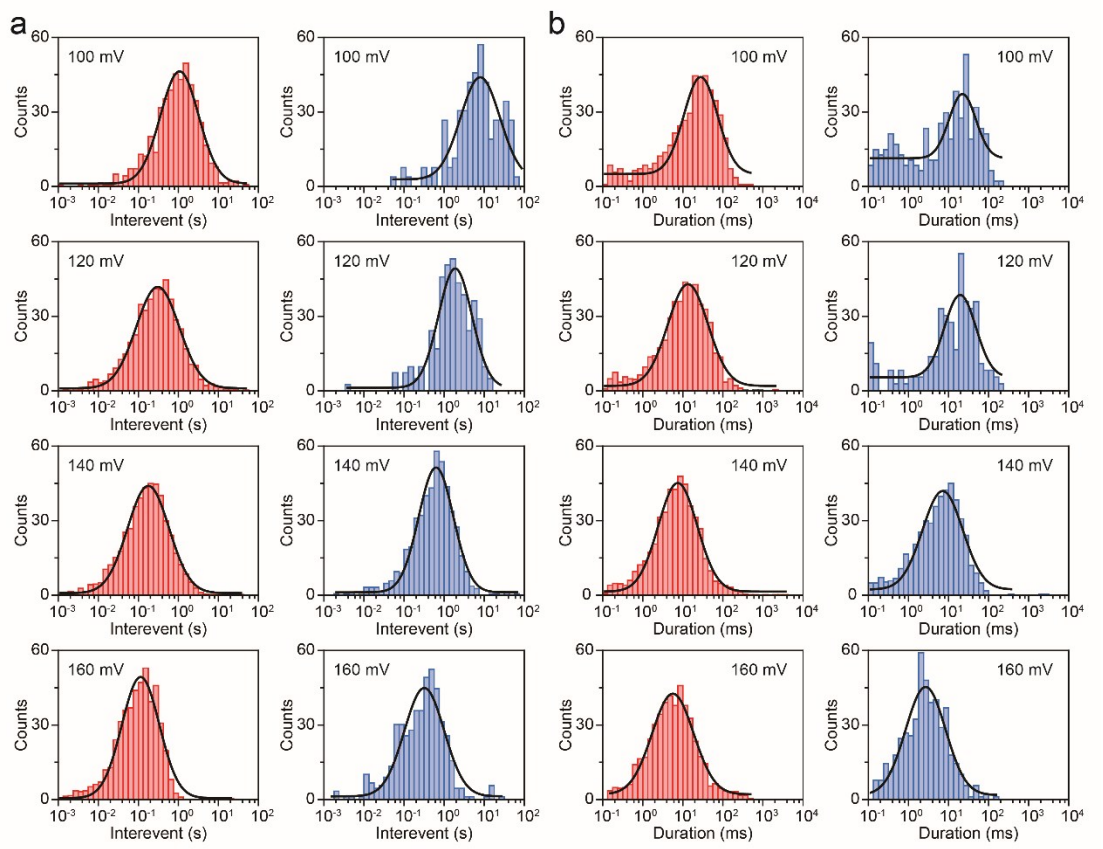

Fig. S3 Histograms of (a) event frequencies and (b) durations for dA_{20} in LiCl (red) and KCl (blue) at various voltages ranging from 100 to 160 mV, respectively (from top to bottom). The duration and frequency distributions are fitted to modified single-exponential functions. Data were obtained in 1.0 M LiCl, 10 mM Tris, 1.0 mM EDTA, pH 8.0 with 2.0 μM dA_{20} in cap side of the aerolysin nanopore.

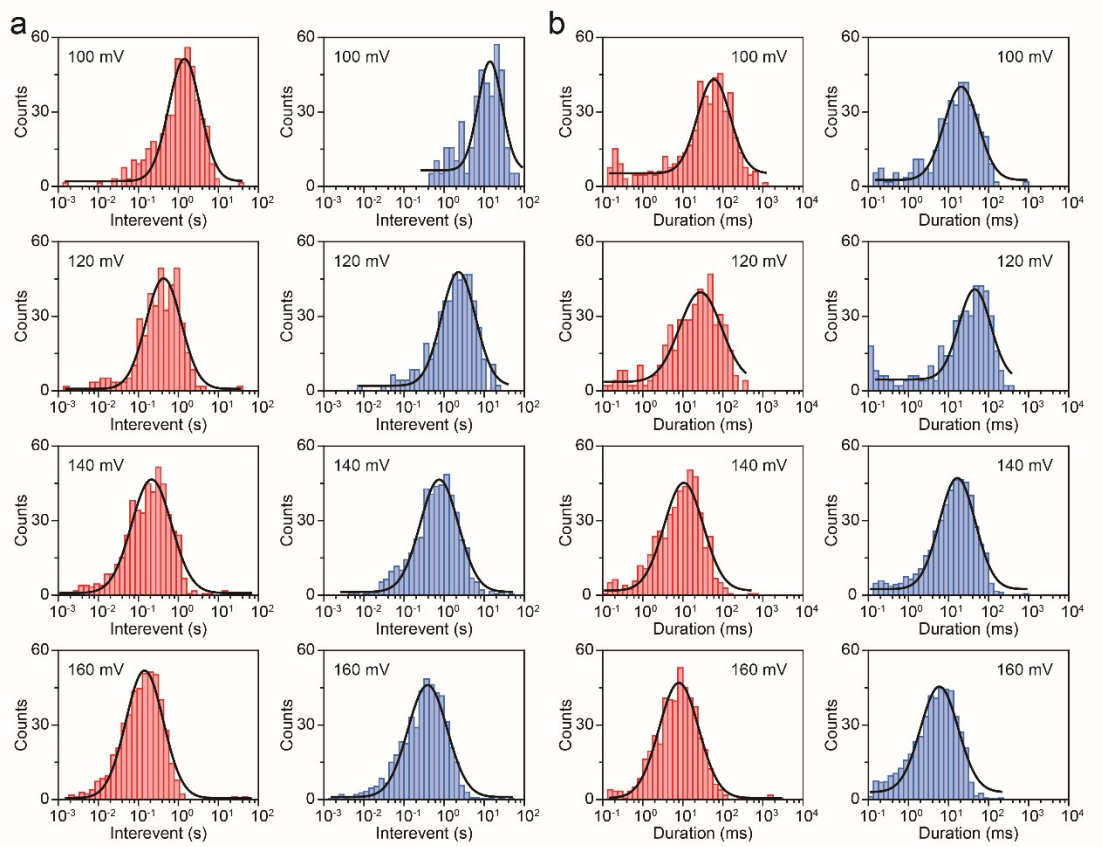

Fig. S4 Histograms of (a) event frequencies and (b) durations for dA_{40} in LiCl (red) and KCl (blue) at various voltages ranging from 100 to 160 mV, respectively (from top to bottom). The duration and frequency distributions are fitted to modified single-exponential functions. Data were obtained in 1.0 M LiCl, 10 mM Tris, 1.0 mM EDTA, pH 8.0 with 2.0 μM dA_{40} in cap side of the aerolysin nanopore.

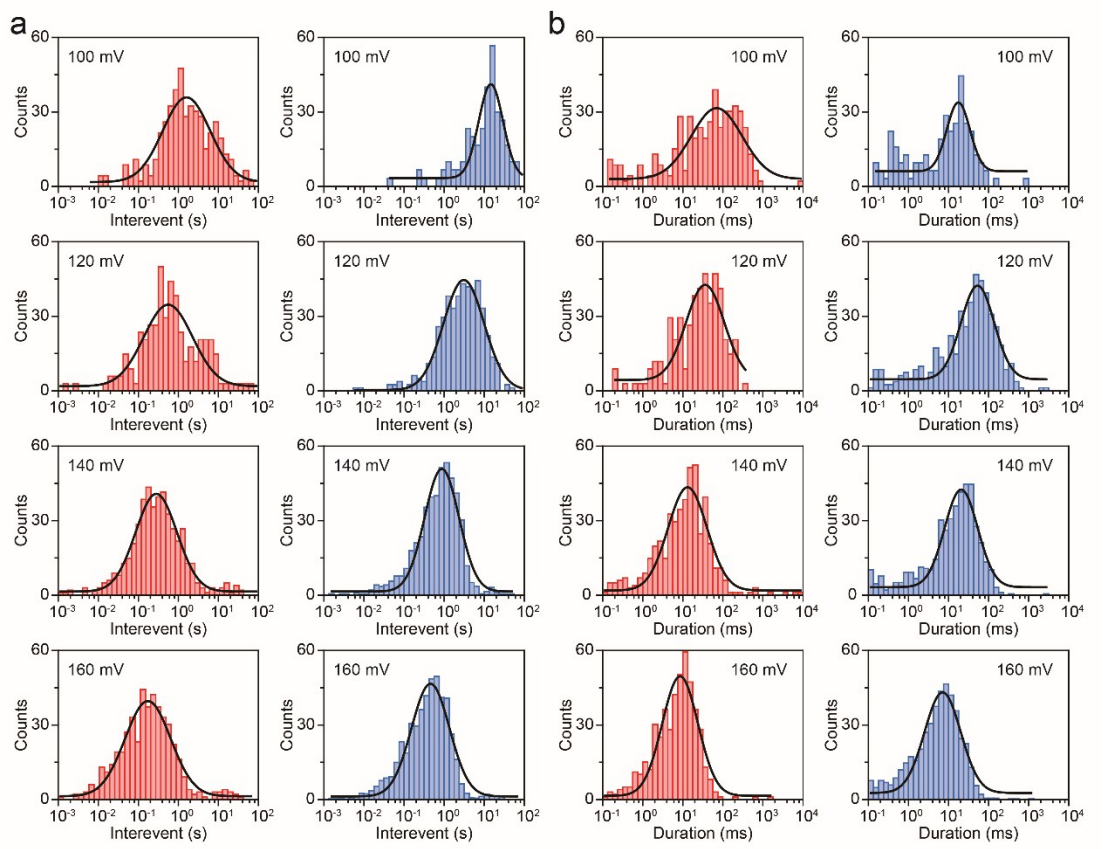

Fig. S5 Histograms of (a) event frequencies and (b) durations for dA_{60} in LiCl (red) and KCl (blue) at various voltages ranging from 100 to 160 mV, respectively (from top to bottom). The duration and frequency distributions are fitted to modified single-exponential functions. Data were obtained in 1.0 M LiCl, 10 mM Tris, 1.0 mM EDTA, pH 8.0 with 2.0 μM dA_{60} in cap side of the aerolysin nanopore.

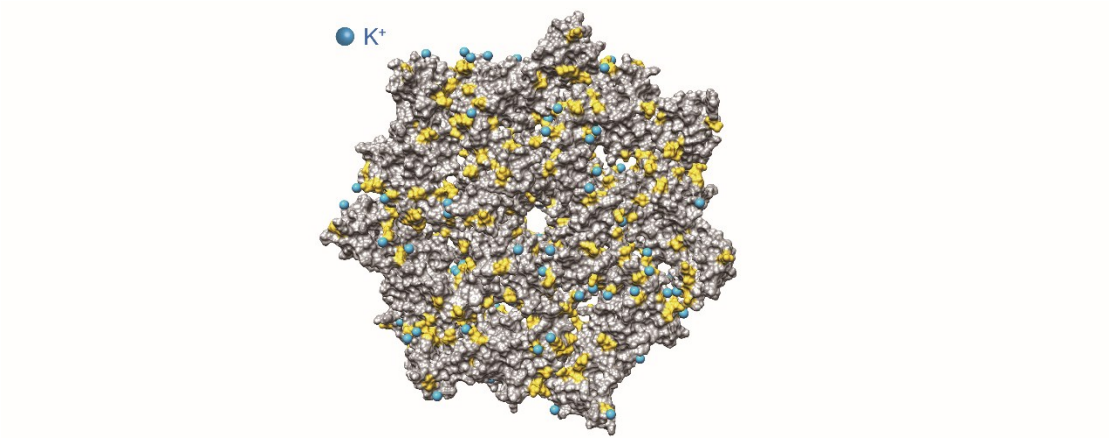

Fig. S6 K^+ bound to AeL in MD simulations. K^+ are represented in blue, the negatively-charged amino acids are shown in yellow and AeL is represented in gray. The illustration is not to scale.

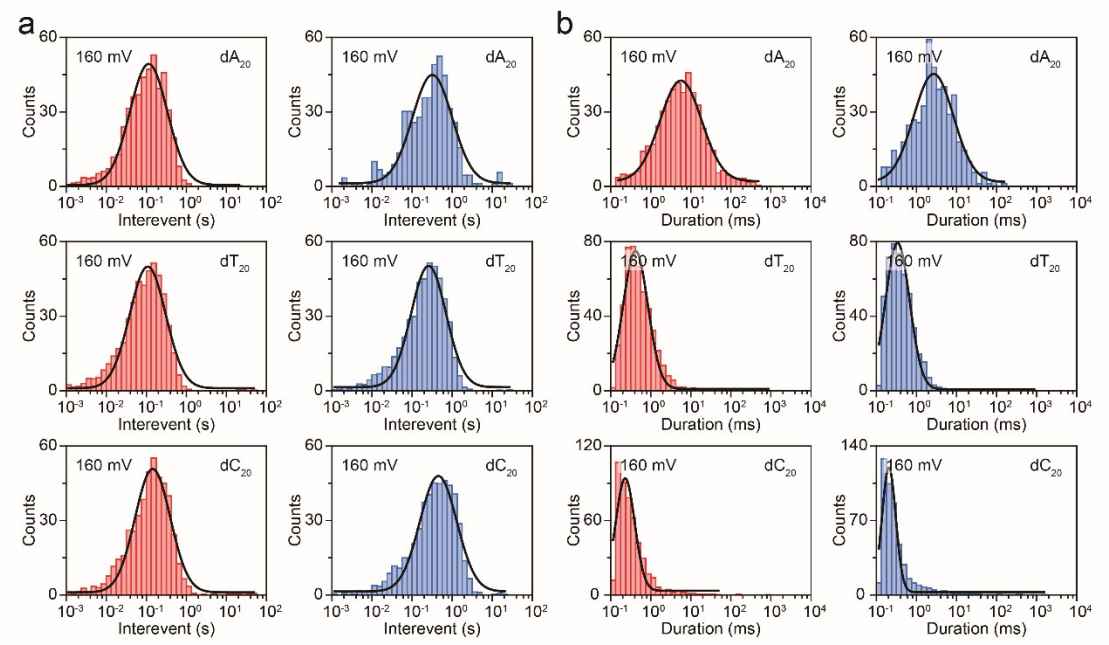

Fig. S7 Histograms of (a) event frequencies and (b) durations for dA_{20}, dT_{20} and dC_{20} in LiCl (red) and KCl (blue) at various voltages ranging from 100 to 160 mV, respectively (from top to bottom). The duration and frequency distributions are fitted to modified single-exponential functions. Data were obtained at + 160 mV (*cis* grounded) in 1.0 M LiCl, 10 mM Tris, 1.0 mM EDTA, pH 8.0 with 2.0 μM ssDNA in cap side of the aerolysin nanopore.

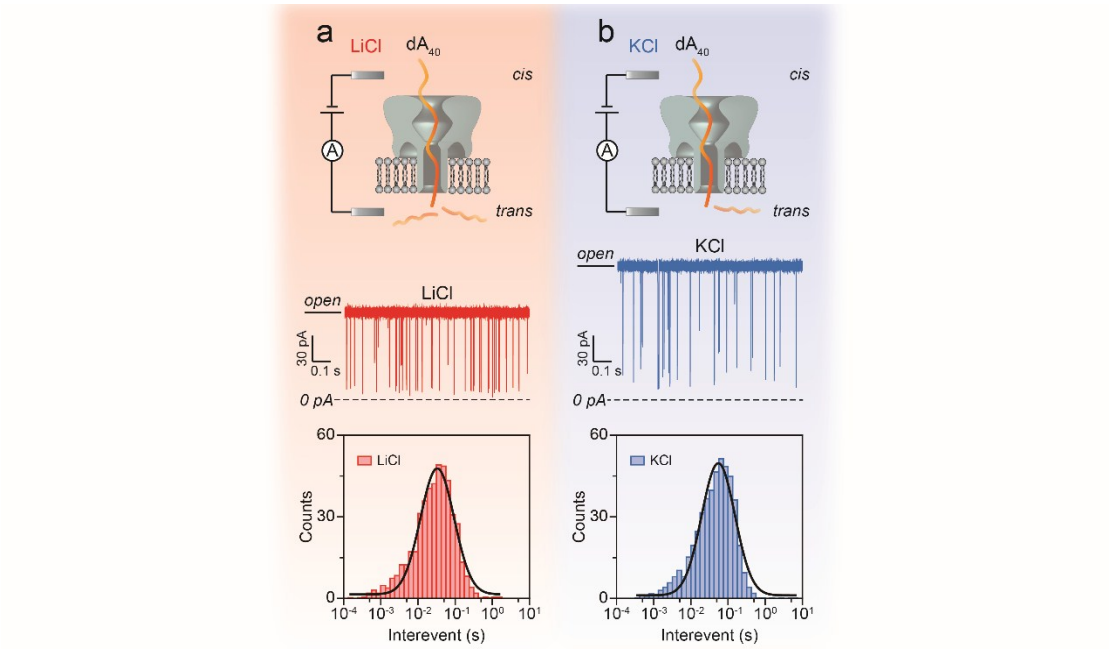

Fig. S8 Detection of dA_{40} via an α-hemolysin (α-HL) nanopore in (a) LiCl and (b) KCl, respectively. The real-time current traces exhibit apparently more frequent blockade events in LiCl than KCl. Data were obtained at + 160 mV (*cis* grounded) in 1 M M^+Cl^- (M^+ = Li^+ or K^+), 1 mM EDTA, 10 mM Tris buffer, pH 8.0 with the presence of 2.0 μM dA_{40} in the cap side of α-HL nanopore.

Supplementary Reference

1 Y. Wang, C. Cao, Y. Ying, S. Li, M. Wang, J. Huang, Y. Long, *ACS Sens.*, 2018, **3**, 779–783.

2 C. Cao, D. Liao, J. Yu, H. Tian and Y. Long, *Nat. Protoc.*, 2017, **12**, 1901–1911.

3 Y. Hu, Y. Ying, Z. Gu, C. Cao and B. Yan, *Chem. Commun.*, 2016, **52**, 5542–5545.

4 Z. Gu, Y. Ying, C. Cao, P. He and Y. Long, *Anal. Chem.*, 2015, **87**, 10653–10656.

5 Z. Gu, Y. Ying, C. Cao, P. He and Y. Long, *Anal. Chem.*, 2015, **87**, 907–913.

6 I. Iacovache, S. De Carlo, N. Cirauqui, M. Dal Peraro, F. G. van der Goot, B. Zuber, *Nat. Commun.*, 2016, **7**, 12062.

7 Y. Wang, M. Li, H. Qiu, C. Cao, M. Wang, X. Wu, J. Huang, Y. Ying, Y. T. Long, *Anal. Chem.*, 2018, **90**, 7790–7794.

8 J. C. Phillips, R. Braun, W. Wang, J. Gumbart, E. Tajkhorshid, E. Villa, C. Chipot, R. D. Skeel, L. Kalé, K. Schulten, *J. Comput. Chem*, 2005, **26**, 1781–1802.

9 A. D. Mackerell, D. Bashford, M. Bellott, R. L. Dunbrack, J. D. Evanseck, M. J. Field, S. Fischer, J. Gao, H. Guo, S. Ha, D. Joseph-McCarthy, L. Kuchnir, K. Kuczera, F. T. K. Lau, C. Mattos, S. Michnick, T. Ngo, D. T. Nguyen, B. Prodhom, W. E. Reiher, B. Roux, M. Schlenkrich, J. C. Smith, R. Stote, J. Straub, M. Watanabe, J. Wiórkiewicz-Kuczera, D. Yin, M. Karplus, *J. Phys. Chem. B*, 1998, **102**, 3586–3616.

10 P. F. Batcho, D. A. Case, T. Schlick, *J. Chem. Phys.*, 2001, **115***,* 4003–4018.

11 S. E. Feller, Y. Zhang, R. W. Pastor, B. R. Brooks, *J. Chem. Phys.*, 1995, **103***,* 4613–4621.

12 A. Aksimentiev and K. Schulten, *Biophys. J.*, 2005, **88**, 3745–3761.

13 W. Humphrey, A. Dalke and K. Schulten, *J. Mol. Graph.*, 1996, **14**, 33–38.

14 S. W. Kowalczyk, D. B. Wells, A. Aksimentiev, C. Dekker, *Nano Lett.*, 2012, **12**, 1038–1044.